Effect of ultrasonication and dispersion stability on the cluster size of alumina nanoscale particles in aqueous solutions

van Son Nguyen, Didier Rouxel, Rachid Hadji, Brice Vincent, Yves Fort

Effect of ultrasonication and dispersion stability on the cluster size of alumina nanoscale particles in aqueous solutions

Van Son Nguyen[1], Didier Rouxel[1], Rachid Hadji[1], Brice Vincent[1], Yves Fort[2]

[1]Institut Jean Lamour - UMR CNRS 7198, Faculté des Sciences et Techniques, Campus Victor Grignard - BP 70239, 54506 VANDOEUVRE-LES-NANCY CEDEX, France
[2] Structure et Réactivité des Systèmes Moléculaires Complexes - UMR CNRS 7565, Faculté des Sciences et Techniques, Campus Victor Grignard - BP 70239, 54506 VANDOEUVRE-LES-NANCY CEDEX, France

Abstract:

This study deals with the deagglomeration of nanoparticles in low concentration suspensions in water, protic polar solvent for polymers such as poly(vinyl alcohol) (PVA). The influence of the main parameters of ultrasonication such as time, power and irradiation modes (continuous, pulsed) on the cluster size of aluminium oxide nanoparticles 1 mg/ml in aqueous solutions was investigated. Power-law dependence of size reduction on ultrasonic time was observed. The study indicated an optimum power input, i.e. at higher vibration amplitude the break up of nanoparticle clusters was no better and there was a risk of reagglomeration occurring during a long ultrasonication. Under optimal conditions, continuous and pulsed irradiations showed almost the same efficiency of deagglomeration over a given time. This result provides alternative operating conditions for attaining the smallest size of the alumina aggregates in suspension.

The influence of stabilisation on the cluster size was also studied. Alumina nanoparticles were stabilized by electrostatic forces against reagglomeration without the need for dispersants, and the enhancement of dispersion stability using electrostatic, steric effects had no significant effect on the aggregate size. On the contrary, the adsorption of high molecular weight polyelectrolytes onto the particle surface could lead to reagglomeration due to material bridges between particle surfaces and even flocculation.

Keywords: aluminium oxide, nanoparticles, dispersion, stabilisation, deagglomeration, ultrasonication

1. Introduction

Due to the improvement of various properties such as mechanical strength, heat resistance and permeability [1, 2], nanocomposites have emerged as a new alternative to neat polymers and conventional composites. More and more new nanoparticles are also synthetized in order to bring specific properties to nanocomposites, such as optical and piezoelectrical properties [3, 4]. However, dispersing fine particles into the polymer matrix homogenously, which allows for taking full advantage of the potential high interface area of the nanofiller-polymer, still remains a challenge. Uniform nanodispersion is essential to ensure transparency and low surface roughness of the nanocomposite, especially for optical applications. Once the quality of the dispersion is sufficient, diffusion light spectroscopies like Brillouin spectroscopy can be used to characterize the mechanical properties of transparent or translucent materials [4]. For such a technique, especially helpful to study the physics of the nanoparticles in liquids or polymers [5], the required size of the samples is

significantly smaller than that for commonly used techniques such as dynamical mechanical analysis (DMA) or conventional mechanical tests [6, 7].

Particle adhesion is caused by surface and field forces (van der Waals, electrostatic and magnetic forces) at direct contact, material bridges between particle surfaces (liquid and solid bridges, flocculants) and interlocking (by macromolecular and particle shape effects) [8]. Once large clusters (agglomerates and aggregates) are generated in the synthesis process, it is very difficult to break them back into primary particles. Aggregates are defined as condensed structures of primary particles, which are held together by solid bridges in various processes such as crystallization, sintering, drying and wet granulation [9]. The term agglomerates relates to looser and more open structures, which can be separated into primary components. Nowadays, ultrasound is well known as an effective way of dispersing nanoparticles homogeneously in suspensions in comparison to other dispersion techniques like ball milling [10], rotor-stator systems [11] and high-pressure nozzle [12]. The ultrasonic dispersion mechanism in media involves acoustic cavitation (formation, growth and implosion of bubbles resulting in the rupture of agglomerates) and acoustic streaming - inducing chaotic mixing. It is worth noting that particle adhesion (especially van der Waals forces) increases when the particle size decreases. Nanoparticles may regroup back into several hundred nanometer clusters shortly after ultrasonication (US) if the suspension is not stabilized enough against reagglomeration. The stabilization may be carried out with electrostatic, steric and electrosteric effects.

Despite the numerous publications on ultrasonic dispersion of nanoparticles in large concentrations in aqueous solutions, relatively little is known about the deagglomeration of nanoparticles in low concentration suspensions. Moreover, nanocomposites based on water-soluble polymers, such as poly(ethylene oxide) (PEO), poly(vinyl alcohol) (PVA), can be prepared directly from aqueous suspensions of nanoparticles. The encapsulation of inorganic nanoparticles with organic layers is also one of the interesting research subjects that lead to the synthesis of nanocomposites. The compatibility of nanoparticles with polymers and non-aqueous solvents can be improved by adsorbing surfactants, particularly polymers, onto the surface of nanoparticles. In this study, we worked on the dispersion of nanoparticles in a protic polar solvent, which corresponds to a model medium for PVA, for example.

In order to produce high quality materials, the dispersion of the smallest clusters in suspension is generally expected. Usually, nanocomposites contain very low quantities of nanosized fillers, but relatively little is known about the deagglomeration of nanoparticles in suspension within this range of concentration. The purpose of this work is to study the influence of the main process parameters, such as time, power and irradiation modes (continuous, pulsed), on the ultrasonic deagglomeration of low concentrations of aluminium oxide nanoparticles in aqueous suspension. The effects of the enhancements of electrostatic repulsion (using pH, ionic strength), steric hindrance (surfactants) and electrosteric stabilisation (polyelectrolytes) on cluster size are also investigated.

2. Experimental

In this work, we are interested in monodisperse suspensions with a very low concentration of nanoparticles. Dispersion experiments were performed in aqueous suspensions of alumina 1 mg/ml. The primary particle size of the nanoparticles used (Aeroxide AluC®, Degussa, Germany) was 13 nm and the specific surface area was 100 m^2/g. The desired solutions were prepared using HNO_3 52.5 % min. (Prolabo), H_2SO_4 95-97 % (Fluka), KNO_3 analytical grade (Acros). Poly(acrylic acid) (PAA), with a molecular weight of 450.000 (Aldrich), and Lutensol FSA 10 (oleic amide ethoxylate - $C_{17}H_{33}CONH(CH_2CH_2O)_{10}H$) (Fluka) were used without further purification.

Transducer Digital Sonifier® Model 450 (Branson Ultrasonics Corporation, USA) was used for generating the ultrasound with a maximum power input of 400 W and a frequency of 20 kHz. The high-frequency voltage output of the generator was transferred into mechanical vibrations by piezoelectric transducers in an exponential horn, with a tip diameter of 13 mm. The vibration amplitude (tip movement) was in the range of 10-65 μm. The power output of the generator could be regulated by adjusting the vibration amplitude. The amount of amplitude (as a percentage of the maximum amplitude) was kept constant by the control electronics of the generator. Ultrasonic exposure could be applied to samples in either continuous or pulsed mode with an intermittence of 0.1-59.9 s. After each experiment, the system measured the energy output of the generator. The specific energy was calculated from the equation:

$$\text{Specific energy}\,(\text{J/cm}^{-3}) = \frac{\text{Energy output (J)}}{\text{Liquid volume}\,(\text{cm}^{-3})}$$

A typical procedure was used to prepare the suspensions: 10 mg of Al_2O_3 and 10 ml of deionized water were placed in a glass container (32 mm diameter, 65 mm height) with a filling level of 15 mm and premixed for 30 minutes with a magnetic stirrer. The solid fraction was 0.03 vol%. The probe tip was immersed 10 mm in solution. Pulsed irradiation with the pulse ratio on/off 0.1/2.0 (s/s) was performed at room temperature without any cooling systems. For the other pulse ratios on/off 0.1/0.1 (s/s), 1.0/1.0 (s/s) and continuous mode, the processing sample was cooled using an ice-water bath. The suspensions were cooled to 1 °C for 15 min before each irradiation. After each ultrasonication, the mean particle size (often given with the symbol Z-average) was measured using dynamic light scattering by a Zetasizer Nano ZS (Malvern Instruments Ltd.). The accumulative active time was used to study the evolution of the mean particle size (depending on experiments, 180 s = 90 s x 2 or 30 s x 6). The Zeta potential of the suspensions was measured using electrophoretic light scattering by the Zetasizer Nano ZS. An average was taken from at least 4 measurements. The error values mentioned in our paper were the repeatability of the measurements. The accuracy must be also taken into account. The accuracy of the measurement of Zeta potential was ±10 %. The pH of the suspensions was measured by a micro-pH 2000 (Crison Instruments SA.).

The morphology of the alumina clusters was characterized by transmission electron microscopy (TEM, Philips CM200). The samples for TEM analysis were prepared by placing a drop of suspension on a carbon film coated copper grid and then dried in air at room temperature.

3. Results and Discussion

3.1. Effects of different parameters of the ultrasonication on nanoparticle cluster size

Preliminary studies on ultrasonication (US) were carried out at room temperature with the pulse ratio on/off 0.1/2.0 (s/s), this ratio allowed the temperature of suspensions at the end of the ultrasonifications to be limited to approximately 30 °C. Particle size distribution (PSD) of alumina suspensions before ultrasonication was bi-modal, which showed the presence of large agglomerates (~5000 nm) and smaller fragments (<1000 nm) (fig. 1). At a relatively low energy input (short processing time – 14 s), large agglomerates were completely broken down into smaller components, which corresponded to a single modal feature of dispersion. As the time progressed, the peak shifted towards the aggregate size.

In fact, the analysis of TEM images of alumina nanoparticles before (fig. 2a) and after ultrasonication (fig. 2b) reveals the solid structure formed from solid bridges between particle surfaces. Fig 2b allows to recognize that the solid bridges between particle surfaces were not broken by ultrasonication. Despite the primary particle size of 13 nm, the hard aggregates

could not be broken into individual nanoparticles under these operating conditions or even at very high energy input [10-12].

Figure 3 presents the evolution of Z-average at the different vibration amplitudes of 10 %, 30 %, 60 %. The mean size of the alumina clusters showed the classical power law dependence on ultrasonic time in relation to the increase of specific energy. The specific energy [13] is a parameter combining both power and time which are the most crucial parameters influencing the deagglomeration. Higher vibration amplitude values should increase the intensity of the bubble collapse and, consequently, the deagglomeration of the nanoparticle clusters [14]. As shown in figure 3, there was a difference in the size reduction of alumina clusters between the vibration amplitudes 10 % and 30 %. As expected, this indicated a lower breakage rate at lower vibration amplitude, i.e. a longer time was necessary to attain the same cluster size.

However, the vibration amplitudes of 30 % and 60 % presented identical values of Z-average to an ultrasonic period of 30 s. Beyond this period, contrary to the theoretical expectations for a vibration amplitude of 60 %, the variations in the cluster sizes followed another trajectory and rose slightly after 300 s of ultrasonication. This result could be explained by the fact that, with the increase of vibration amplitude, bubbles may grow so large that the time available in the adjacent rarefaction cycle will not be sufficient for them to collapse [13], hence reducing cluster breakage. Similar reagglomeration was also reported elsewhere [15, 16]; the coarsening of the clusters is related to the capillary pressure of the system due to the high surface tension of the water and/or by the hydrogen bonds of the surface hydroxyl groups [16].

With the pulse ratio on/off 0.1/2.0 (s/s), the operative duration was long because the inactive time was 20 times greater than the active. To reduce the duration of ultrasonication, greater pulse frequency and continuous irradiation were considered. The samples were immersed in an ice-water bath (1 °C) to resolve the heating problems. Process temperature is also an important parameter of ultrasonic efficiency. With increasing temperature, less energy can be brought into the fluid [17]. A maximum efficiency of ultrasound energy conversion to particle breakage is calculated using calorimetry at about 25 °C [18]. The smaller the volume, the more difficult the cooling procedure becomes. From the data listed in table 1, one can see that the temperature at the end of ultrasonication rose with vibration amplitude and exposure time (increasing specific energy) but did not exceed 24 °C for all powers applied. One should notice that a simple ice-water bath provided sufficient cooling (< 25 °C) for 10 ml suspension samples.

As can be seen from figure 4, at 30 % vibration amplitude, the alumina nanoparticle size showed no difference in any of the modes of ultrasonic irradiation used in spite of different amounts of specific energy (table 1). This result should be emphasized because previous studies have shown that sonochemistry using pulses is generally less effective than continuous irradiation [19-21]. It seems that in most of our experiments, the applied specific energy exceeded that needed for deagglomaration, but did not overcome the disaggregation energy. After 180 s of ultrasonication, the smallest attainable size was about 150 nm. A similar value has also been reported in literature [13, 22], showing that the aggregate size was dominated by the particle type rather than the operating conditions. Furthermore, prolonged ultrasonication can result in a contamination of the dispersion due to ultrasonic horn erosion [15].

The effect of vibration amplitude with the pulse ratio 0.1/0.1 (s/s) and continuous irradiation on the cluster size is shown in figure 5. The increase in specific energy by increasing the vibration amplitude of the ultrasonic field should improve break up efficiency. Our studies revealed the most effective deagglomeration of nanoparticle clusters at 30 % vibration amplitude. Higher vibration amplitude did not show any improvement in the

deagglomeration. Pulsed ultrasonic irradiation at 30 % and 60 % gave almost the same results (fig. 5a), whereas in the continuous mode, the results at 10 % and 60 % were almost identical, and less efficient than at 30% (fig. 5b). At 60 % vibration amplitude, the continuous mode was visually observed to cause more powerful acoustic streaming than pulsed irradiation but produced less breakage. Higher acoustic streaming could be explained by the fact that the fluid flows caused by ultrasound had more time to relax in the pulsed irradiation than in continuous mode. Thus, the intensity of the fluid flows in continuous mode was more significant. Higher fluid flows might reduce the ultrasonic breakage efficiency. Indeed, Raman et al. [18] reported that particle breakage is more prominent at lower flow rates.

In conclusion, the mean size of alumina clusters decreased by increasing ultrasonic time and vibration amplitude. However, the results indicated an optimal deagglomeration efficiency at 30 % vibration amplitude after 180 s of ultrasonication. The increase in specific energy input using higher vibration amplitude or prolonged irradiation lead to insignificant size reduction and sometimes even the reagglomeration of the nanoparticles. Thus, ultrasonication at 30 % vibration amplitude with different modes of irradiation will be used to investigate the influence of dispersion stability on cluster size.

3.2. Influence of dispersion stability on clusters size

In liquids, especially in aqueous solutions, the dissociation of surface groups of alumina generates electric charges on the surface of nanoparticles. The stability of colloidal suspensions is mostly governed by interparticle (or surface) forces [23], especially by the repulsive electrostatic interaction of these charges. Clearly, surface modifications (e.g. by changing the pH, adding inert electrolytes or the adsorption of surfactants, polyelectrolytes) can alter the particle-particle interactions and, consequently, the stability of the suspensions [24, 25].

3.2.1. Electrostatic repulsion

The isoelectric point (IEP) of alumina is found to be above pH 8 [26-28]. Below the IEP, protonated hydroxyl groups of alumina ($Al\text{-}OH_2^+$) dominate the positive charge of the surface (fig. 9). Above the IEP, the negative charges result from the formation of $Al\text{-}O^-$ groups. Previous studies have shown that the maximum Zeta potential is obtained at pH 2 [25-27]. In this study, the natural pH of the alumina 1 mg/ml suspension occurred at 7.3. At this pH, the Zeta potential of the suspension was 33 mV and the particles were stabilized by electrostatic forces against reagglomeration.

The addition of salt caused large agglomerates, which were easily disrupted by ultrasound (fig. 6). As can be seen in table 2 and figure 6, increasing the Zeta potential from 33 mV to about 51 mV by changing the pH and/or adding salt (improving ionic strength) had no significant influence on ultrasonic deagglomeration of nanoparticle clusters. Similar to the break up of TiO_2 nanoparticles in electrostatically stabilized suspensions [15], none of the nanopowders was successfully broken down to their primary particles.

Surprisingly, in the solution of H_2SO_4 at pH 2 (fig. 7), shortly after the end of ultrasonication, alumina nanoparticles reformed back into large agglomerates. The suspension was cloudier than the other suspensions and the flocs completely settled to the bottom of the liquid within 30 minutes. This is due to the approximately zero Zeta potential (table 2). Anion SO_4^{2-} adsorbed and neutralized positive charges on the surfaces of two or more colloidal particles, bound them together, giving flocculation.

Lastly, the improvement of electrostatic repulsion did not bring about a significant change in mean cluster size. On the other hand, the adsorption of electrolyte ions on the nanoparticle surface, especially at high electrolyte strengths, could lead to the bridging of nanoparticles [25, 29] or flocculation.

3.2.2. Steric and electrosteric stabilization

3.2.2.1.Steric stabilization

Another traditional method to prevent flocculation of particles is adsorption of a dispersant layer (adlayer) around the particle surface. An adlayer with the appropriate thickness can stabilize the particles against the attractive van der Waals forces through mechanisms such as steric hindrance. In this study, steric stabilisation was performed in suspensions of Lutensol, which is used in miniemulsion polymerization [30, 31] and heavy metal ion sorption [32, 33]. Lutensol possesses a long chain alkyl tail (18 carbons) and a -C_2H_4O- head group able to anchor itself strongly onto the surface of the nanoparticle.

This study shows that, like the enhancement of electrostatic stabilization, the suspension stability of Lutensol has little effect on cluster size (fig.8). In fact, the Z-average varies around the size of the aggregates. The results can be explained by the fact that the carbon chains (C-18) of the surfactant are not long enough to provide the required adlayer thickness for true steric stability [34, 35]. On the other hand, the Zeta potential of suspensions were in the range of 40 mV. As was mentioned previously, electrostatic forces could influence the stability of Al_2O_3 nanoparticles in aqueous suspensions. With increasing surfactant concentration, the material bridge between particle surfaces had a greater tendency to form larger agglomerates.

3.2.2.2.Electrosteric stabilization

Polyelectrolytes have been used to impact the stability of particles via an electrosteric mechanism. Adsorption of these charged molecules onto the particle surface will alter the surface charge and hence the Zeta potential [25]. By increasing the adlayer thickness, steric hindrance increases and stabilizes the suspension. In the case of poly(acrylic acid), the thickness of the adsorption layer increases with an increase in its molecular weight, concentration and a decrease in the pH [27, 36, 37].

The pH of Al_2O_3/PAA suspensions was in the range of 6-7.5. The pK_a of PAA is known to be about 4.5. In the pH range 4.5-8 (IEP of Al_2O_3 >8), apart from hydrogen bonding, chemical interaction between carboxylate ions ($-COO^-$) and $Al-OH_2^+$ species can take place [38] (fig. 9). This causes a reduction in the surface charge of the colloids. Consequently, the Zeta potential decreases almost linearly with the PAA concentration before attaining the value maxima about -40 mV at 40 mg/l of the surfactant (fig. 10). This is probably related to the optimum adsorbed amount of PAA about 0.4 mg/m^2 [25]. A similar phenomenon has been reported for the suspensions of PAA/TiO_2 nanoparticles [36].

With the absolute values of the Zeta potential less than 30 mV, the attractive forces between the colloids were stronger than the repulsive forces. Moreover, below the optimum dispersant concentration, nanoparticle surfaces were not fully covered by surfactant, so the adlayer was not thick enough to prevent reagglomeration. Thus, obvious flocculation occurred for the systems of PAA 10-30 mg/l. The light scattering results shown in figure 11 revealed a peak of large agglomerates, which had a mean diameter of about 5000 nm, in the suspension with 30 mg/l of PAA. From 40 mg/l of PAA, the colloidal systems were stabilized by the electrosteric effect of the protective layer. However, from the data listed in table 3, mean cluster sizes were greater than the value obtained without the dispersant and increased with the concentration of PAA. This is related to the fact that polymers of high molecular weight, adsorbed simultaneously on two or more neighbouring surfaces of the particles will cause them to combine together, forming agglomerates. In addition, an excess of surfactant can cause reagglomeration due to bridging or the depletion effect [29].

Under the conditions of our study, the suspension stability predominantly depended on electrostatic repulsion. In the presence of Lutensol, steric stabilization had a little effect on

cluster size. By contrast, the adsorption of PAA onto a particle surface strongly affected the Zeta potential of the nanoparticles. As a result, non-stabilized nanoparticles tended to flocculate. However, concentration of PAA higher than 40 mg/l led to larger clusters, which was interpreted as reagglomeration due to bridging or the depletion effect. In all our experiments, continuous and pulsed ultrasonication did not show any marked difference in deagglomeration despite the breakage of the hydrogen bonding networks for Al_2O_3 and PAA during ultrasonic exposure [39].

4. Conclusion

To sum up, the aggregate size (the smallest attainable size) of alumina nanoparticles at low concentration in aqueous suspensions could be reached by several ultrasonic processing deagglomerations with either continuous or pulsed irradiation. Experimental results showed the optimal break up efficiency at a vibration amplitude of 30 %. Higher vibration amplitude showed no improvement in the breakage process, moreover prolonged ultrasonication could result in the reagglomeration of nanoparticles.

During the ultrasonic deagglomeration, alumina particles at low concentration in suspensions were stabilized by electrostatic forces without the need for dispersants. The improvement of electrostatic repulsion and adsorption of surfactants onto particle surfaces did not have a significant influence on the aggregate size. Nevertheless, in appropriate conditions, the encapsulation of nanoparticles by adsorbing polymers is of interest in the preparation of nanocomposites.

Acknowledgment

This work was funded by the French National Agency for Research (N° ANR-08-NANO-041) and labelled by the French competitiveness clusters PLASTIPOLIS and MATERALIA.

References

[1] S.S. Ray, M. Okamoto, Polymer/layered silicate nanocomposites: a review from preparation to processing, Prog. Polym. Sci. 28 (2003) 1539-1641.
[2] D.R. Paul, L.M. Robeson, Polymer nanotechnology: Nanocomposites, Polymer 49 (2008) 3187-3204.
[3] M. Aufray, S. Menuel, Y. Fort, J. Eschbach, D. Rouxel, B. Vincent, New synthesis of nano-sized niobium oxides and lithium niobate particles and their characterization by XPS analysis, J. Nanosci. Nanotechnol. 9 (2009) 4780-4785.
[4] J. Eschbach, D. Rouxel, B. Vincent, Y. Mugnier, C. Galez, R.L. Dantec, P. Bourson, J.K. Krüger, O. Elmazria, P. Alnot, Development and characterization of nanocomposite materials, Mater. Sci. Eng., C 27 (2007) 1260-1264.
[5] D. Rouxel, J. Eschbach, B. Vincent, R. Kouitat, Nanocomposites PMMA/SiO2: Brillouin scattering and tribological study. Names 3rd France-Russia Seminar 2007, pp. 79 - 82.
[6] B. Vigolo, B. Vincent, J. Eschbach, P. Bourson, J.F. Mareche, E.M. Rae, A. Muller, A. Soldatov, J.M. Hiver, A. Dahoun, D. Rouxel, Multiscale characterization of single-walled carbon nanotube/polymer composites by coupling Raman and Brillouin spectroscopy, J. Phys. Chem. C 113 (2009) 17648-17654.
[7] J.K. Krüger, U. Müller, R. Bactavatchalou, J. Mainka, C. Gilow, W. Possart, A. Tschöpe, P. Alnot, D. Rouxel, R. Sanctuary, B. Wetzel, The generalized Cauchy relation as an universal property of the amorphous state, J. of Phys. IV 129 (2005) 45-49.
[8] J. Tomas, Adhesion of ultrafine particles—A micromechanical approach, Chem. Eng. Sci. 62 (2007) 1997 – 2010.

[9] A.P. Tinke, R. Govoreanu, I. Weuts, K. Vanhoutte, D.D. Smaele, A review of underlying fundamentals in a wet dispersion size analysis of powders, Powder Technol. 196 (2009) 102-114.
[10] S. Kimitoshi, L. Ji-Guang, K. Hidehiro, I. Takamasa, Ultrasonic Dispersion of TiO_2 Nanoparticles in Aqueous Suspension, J. Am. Ceram. Soc. 91 (2008) 2481-2487.
[11] M. Pohl, H. Schubert, Dispersion and de-agglomeration of nanoparticles in aqueous solutions. International Congress for Particle Technology Partec 2004, Nuremberg, Germany, 2004.
[12] J. Baldyga, L. Makowski, W. Orciuch, C. Sauter, H.P. Schuchmann, Deagglomeration processes in high-shear devices, Chem. Eng. Res. Des. 86 (2008) 1369-1381.
[13] C. Sauter, M.A. Emin, H.P. Schuchmann, S. Tavman, Influence of hydrostatic pressure and sound amplitude on the ultrasound induced dispersion and de-agglomeration of nanoparticles, Ultrason. Sonochem. 15 (2008) 517–523.
[14] T.J. Mason, J.P. Lorimer, Applied sonochemistry, Wiley-VCH, Weinheim, 2002.
[15] N. Mandzy, E. Grulke, T. Druffel, Breakage of TiO_2 agglomerates in electrostatically stabilized aqueous dispersions, Powder Technol. 160 (2005) 121 – 126.
[16] O. Vasylkiv, Y. Sakka, Synthesis and colloidal processing of zirconia nanopowder, J. Am. Ceram. Soc. 84 (2001) 2489–2494.
[17] J.-M. Löning, C. Horst, U. Hoffmann, Investigations on the energy conversion in sonochemical processes, Ultrason. Sonochem. 9 (2002) 169-179.
[18] V. Raman, A. Abbas, Experimental investigations on ultrasound mediated particle breakage, Ultrason. Sonochem. 15 (2008) 55-64.
[19] A. Henglein, M. Gutierrez, Sonochemistry and sonoluminescence: effects of external pressure, J. Phys. Chem. 97 (1993) 158-162.
[20] A. Henglein, Chemical effects of continuous and pulsed ultrasound in aqueous solutions, Ultrason. Sonochem. 2 (1995) 115-121.
[21] M. Cutierrez, A. Henglein, Chemical action of pulsed ultrasound: observation of an unprecedented intensity effect, J. Phys. Chem. 94 (1990) 3625-3628.
[22] N.G. Özcan-Taskin, G. Padron, Effect of particle type on the mechanisms of break up of nanoscale particle clusters, 13th European Conference on Mixing (2009) 14-17.
[23] A.L. Jennifer, Colloidal processing of ceramics, J. Am. Ceram. Soc. 83 (2000) 2341-2359.
[24] V.M. Gun'ko, V.I. Zarko, R. Leboda, E. Chibowski, Aqueous suspension of fumed oxides: particle size distribution and zeta potential, Adv. Colloid Interface Sci. 91 (2001) 1-112.
[25] R. Greenwood, Review of the measurement of zeta potentials in concentrated aqueous suspensions using electroacoustics, Adv. Colloid Interface Sci. 106 (2003) 55-81.
[26] S. Boufi, Baklouti, S., Pagnoux, C., Baumard, J.-F., Interaction of cationic and anionic polyelectrolyte with SiO_2 and Al_2O_3 powders, J. Eur. Ceram. Soc. 17 (1997) 1387-1392.
[27] O. Lyckfeldt, L. Palmqvist, E. Carlström, Stabilization of alumina with polyelectrolyte and comb copolymer in solvent mixtures of water and alcohols, J. Eur. Ceram. Soc. 29 (2009) 1069-1076.
[28] A. Schrijnemakers, S. André, G. Lumay, N. Vandewalle, F. Boschini, R. Cloots, B. Vertruyen, Mullite coatings on ceramic substrates: Stabilisation of Al_2O_3–SiO_2 suspensions for spray drying of composite granules suitable for reactive plasma spraying, J. Eur. Ceram. Soc. 29 (2009) 2169-2175.
[29] A.R. Studart, E. Amstad, L.J. Gauckler, Colloidal stabilization of nanoparticles in concentrated suspensions, Langmuir 23 (2007) 1081-1090.

[30] K. Landfester, N. Bechthold, F. Tiarks, M. Antonietti, Miniemulsion polymerization with cationic and nonionic surfactants: a very efficient use of surfactants for heterophase polymerization, Macromolecules 32 (1999) 2679-2683.
[31] C. Stubenrauch, R. Tessendorf, R. Strey, I. Lynch, K.A. Dawson, Gelled polymerizable microemulsions. 1. phase behavior, Langmuir 23 (2007) 7730-7737.
[32] J. Snukiškis, D. Kaušpėdienė, Integrated removal of nonionic surfactant and cobalt(II) from plating rinse water, Colloids Surf., A 253 (2005) 27-32.
[33] R. Jancevičiute, A. Gefeniene, Sorption of copper (II) and nonionic surfactant by ion exchangers and activated carbon, J. Environ. Eng. Landsc. Manag. 14 (2006) 191-197
[34] R.E. Johnson, W.H. Morrison, Ceramic powder dispersion in nonaqueous systems in: G.L. Messing, K.S. Mazdiyasni, J.W. McCauley, R.A. Haber (Eds), Advanced Ceramics American Ceramic Society, Westerville, Ohio, 1987, pp. 323-348.
[35] A.R. Studart, E. Amstad, M. Antoni, L.J. Gauckler, Rheology of concentrated suspensions containing weakly attractive alumina nanoparticles, J. Am. Ceram. Soc. 89 (2006) 2418–2425.
[36] S. Liufu, H. Xiao, Y. Li, Adsorption of poly(acrylic acid) onto the surface of titanium dioxide and the colloidal stability of aqueous suspension, J. Colloid Interface Sci. 281 (2005) 155-163.
[37] S. Farrokhpay, A review of polymeric dispersant stabilisation of titania pigment, Adv. Colloid Interface Sci. 151 (2009) 24-32.
[38] D. Santhiya, S. Subramanian, K.A. Natarajan, S.G. Malghan, Surface chemical studies on the competitive adsorption of poly(acrylic acid) and poly(vinyl alcohol) onto alumina, J. Colloid Interface Sci. 216 (1999) 143–153.
[39] L.N. Ngo, T. Kobayashi, Ultrasound stimulus effect on hydrogen bonding in networked alumina and polyacrylic acid slurry, Ultrason. Sonochem. 17 (2010) 186-192.

Figures and tables:

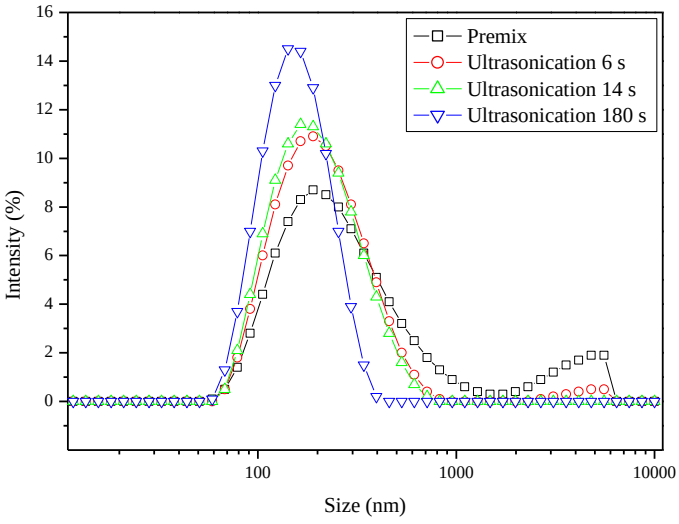

Figure 1: Particles size distribution by intensity of alumina in ultrasonic deagglomeration at 30 % vibration amplitude.

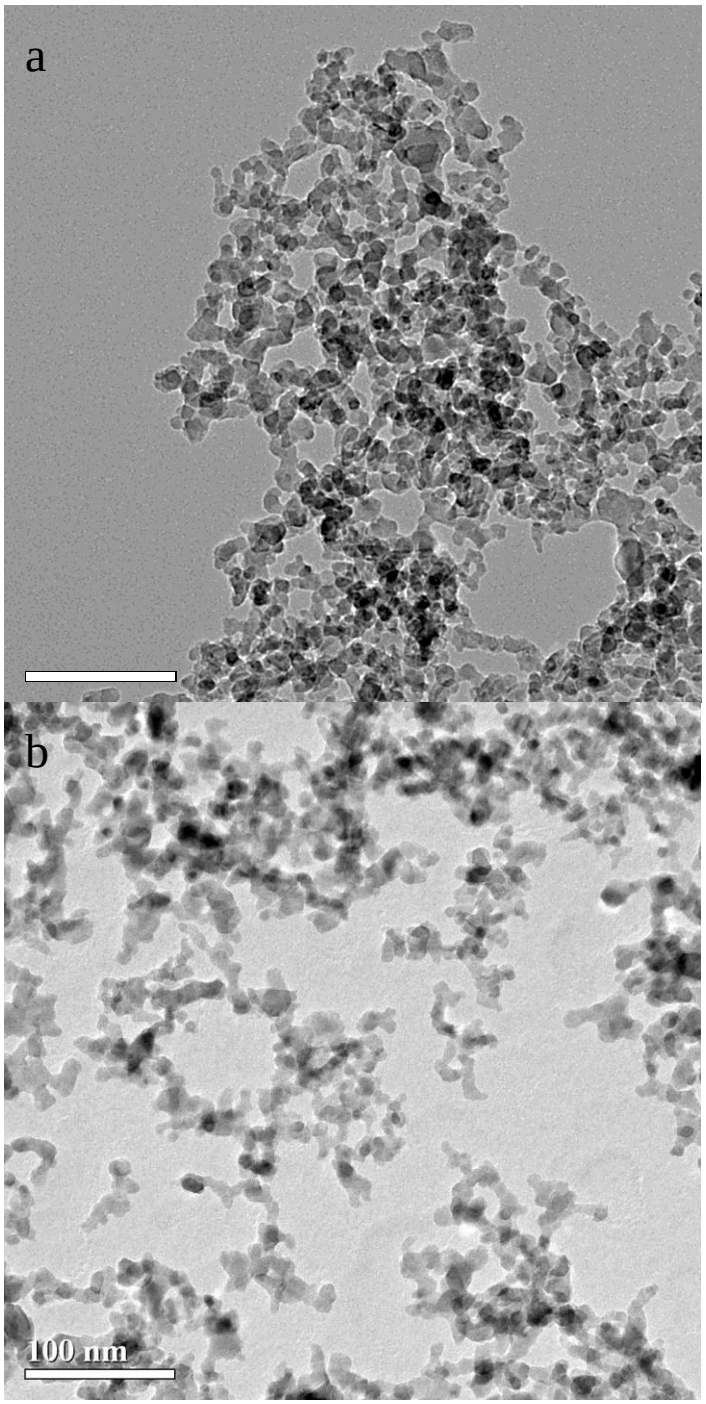

Figure 2 : TEM images of alumina nanoparticles (a) before and (b) after 180 s of ultrasonication at 30 % vibration amplitude.

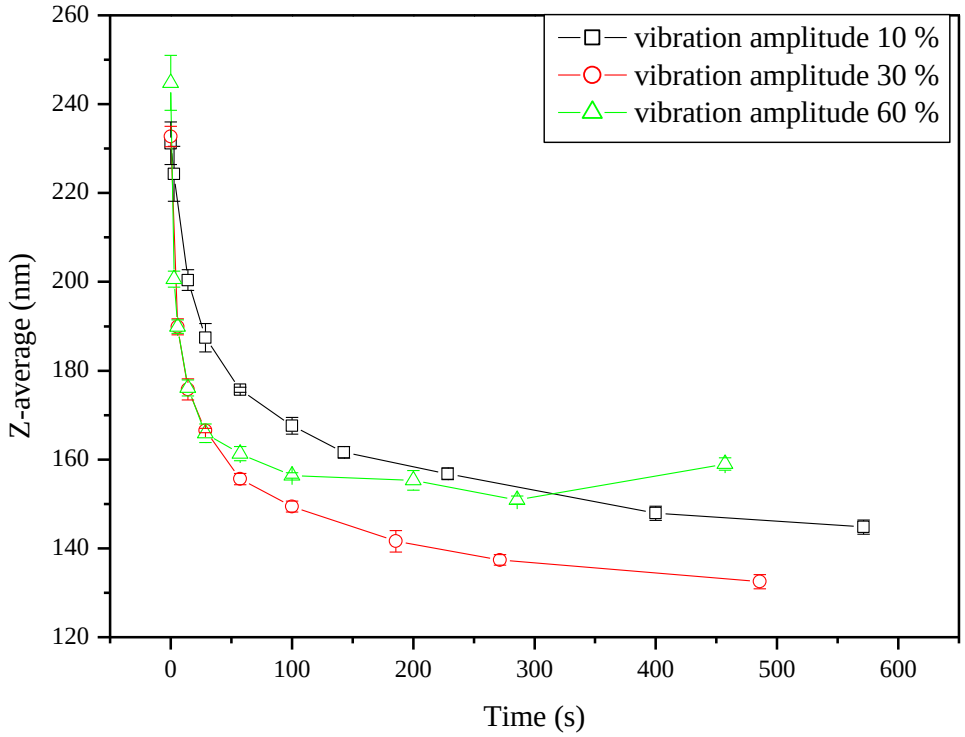

Figure 3: Evolution of mean alumina nanoparticle size at different vibration amplitudes of 10 %, 30 %, 60 % versus ultrasonic time (pulse ratio 0.1/2.0 (s/s)).

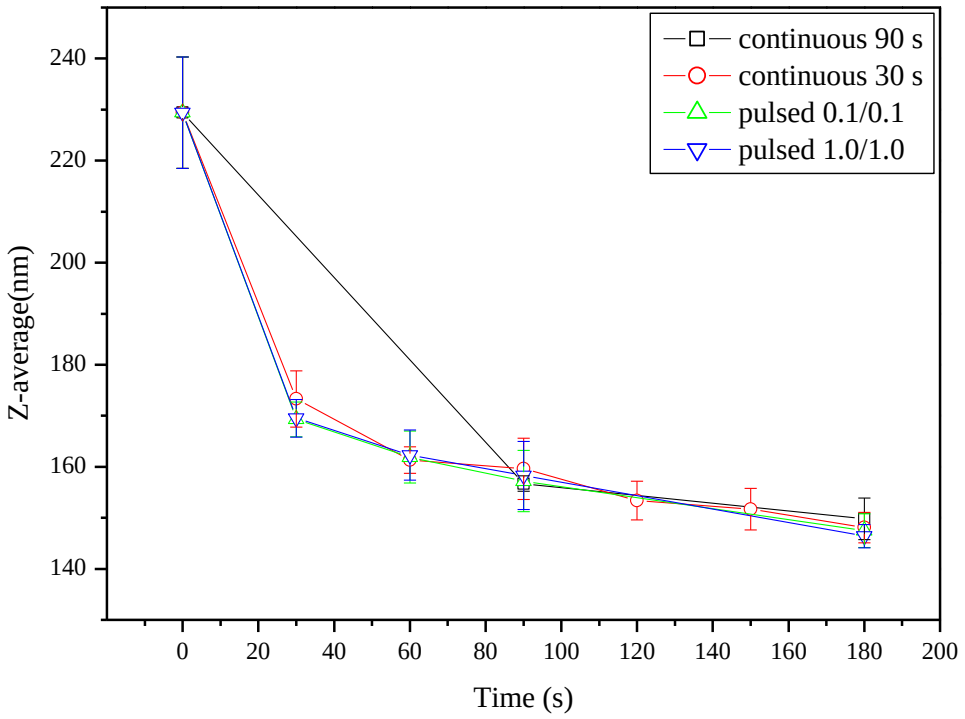

Figure 4 : Influence of ultrasonic modes (continuous and pulsed) on the deagglomeration of alumina nanoparticle at 30 % vibration amplitude.

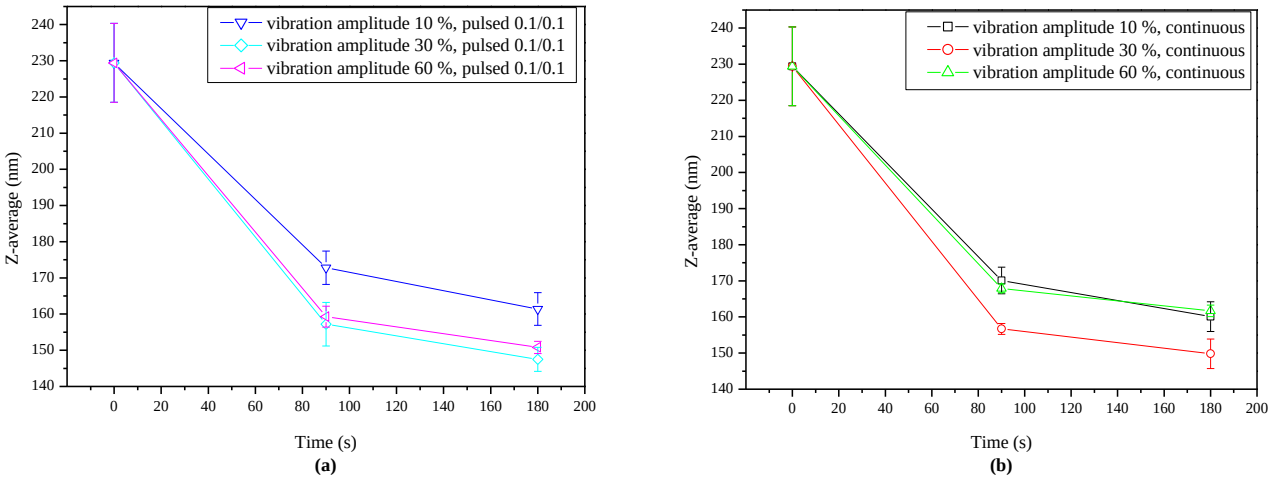

Figure 5 : Influence of vibration amplitude of ultrasound on the deagglomeration of alumina nanoparticles (a) radiation with pulse ratio 0.1/0.1 (s/s) and (b) continuous mode.

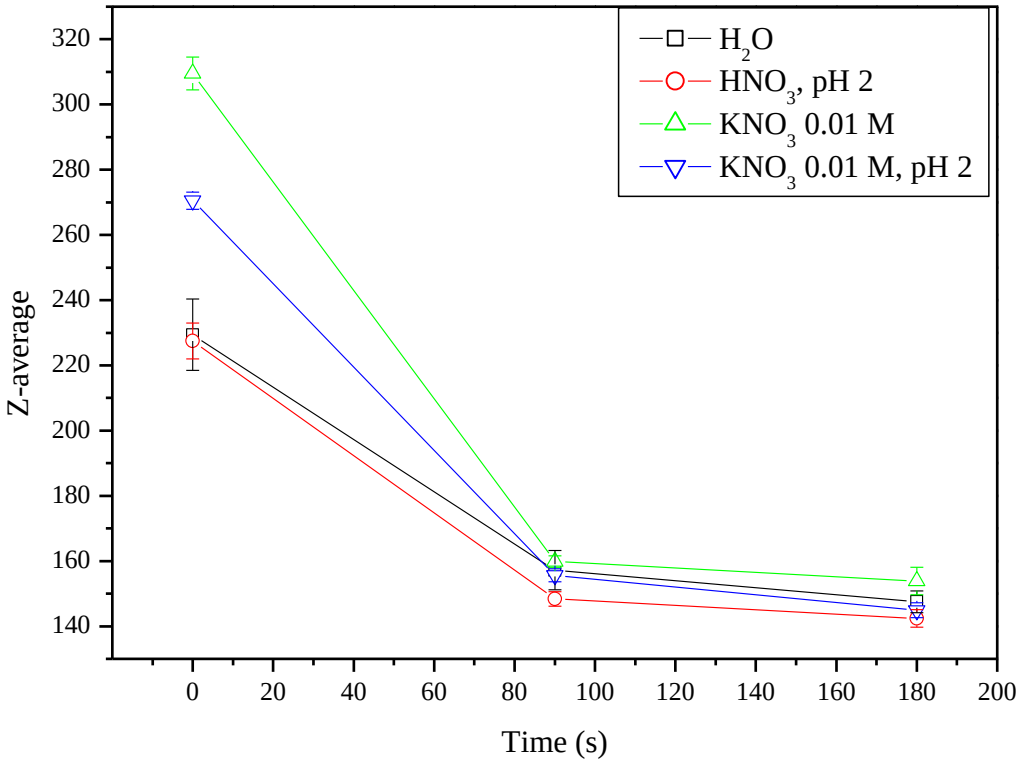

Figure 6 : Evolution of mean alumina nanoparticle size in different suspensions versus ultrasonic time.

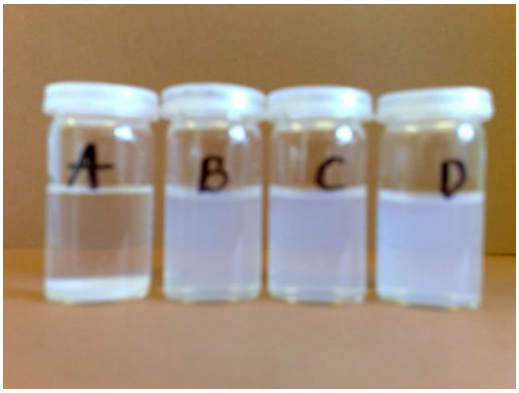

Figure 7: Alumina suspensions after ultrasonication 30 min (A) pH 2, H_2SO_4 ; (B) pH 2, HNO_3; (C) KNO_3 0.01 M; (D) pH 2, HNO_3 and KNO_3 0.01 M.

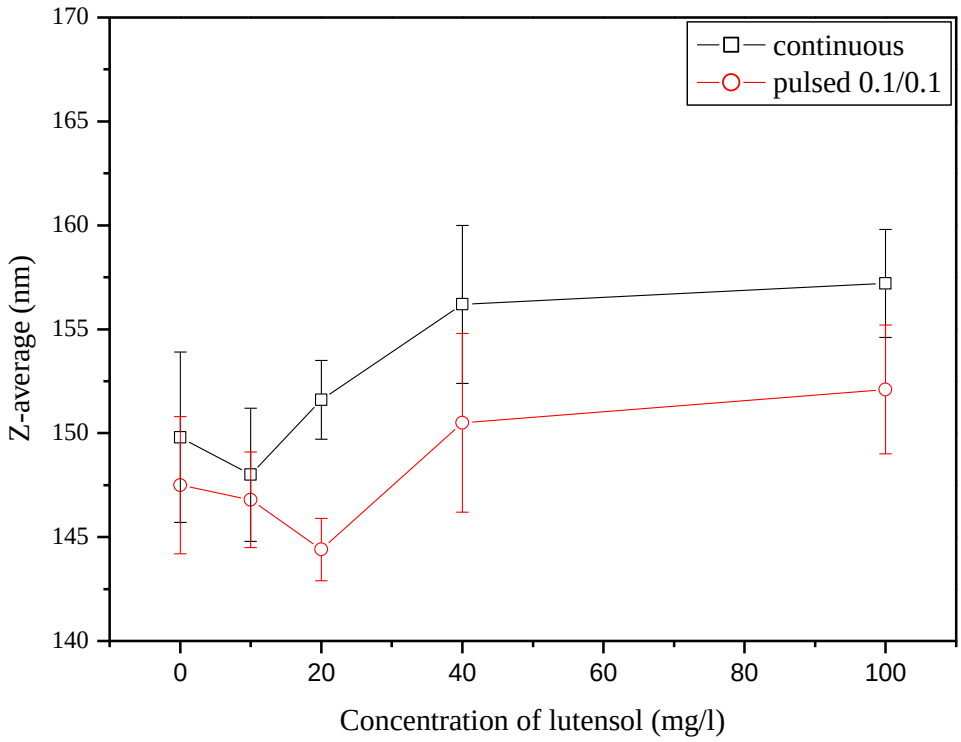

Figure 8 : Influence of Lutensol concentration on mean alumina nanoparticle size after 180 s of ultrasonication.

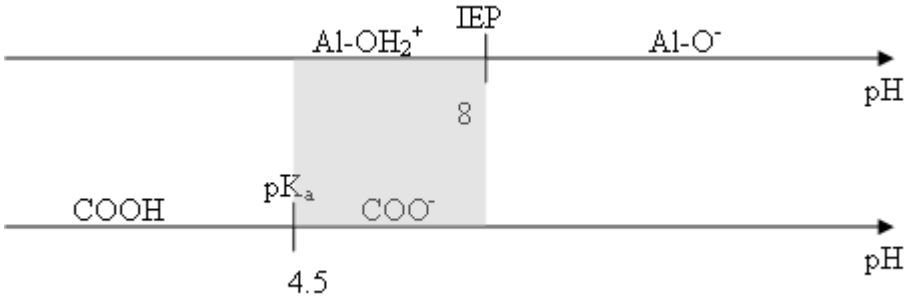

Figure 9: Surface groups of alumina and carboxyl groups of PAA in various pH of solution.

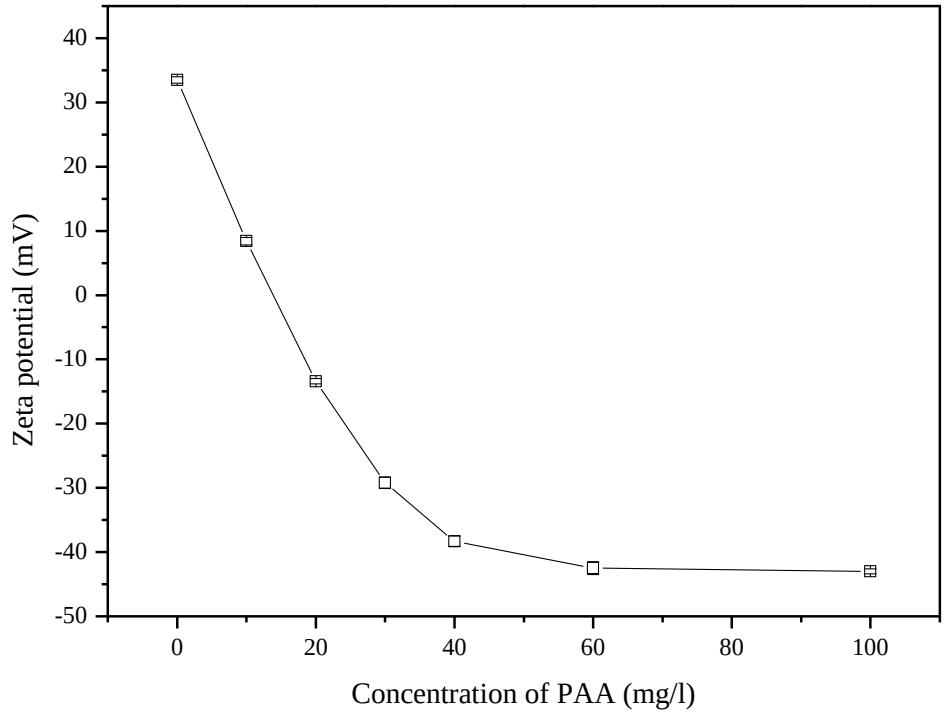

Figure 10 : Influence of PAA concentration on Zeta potential of alumina nanoparticles.

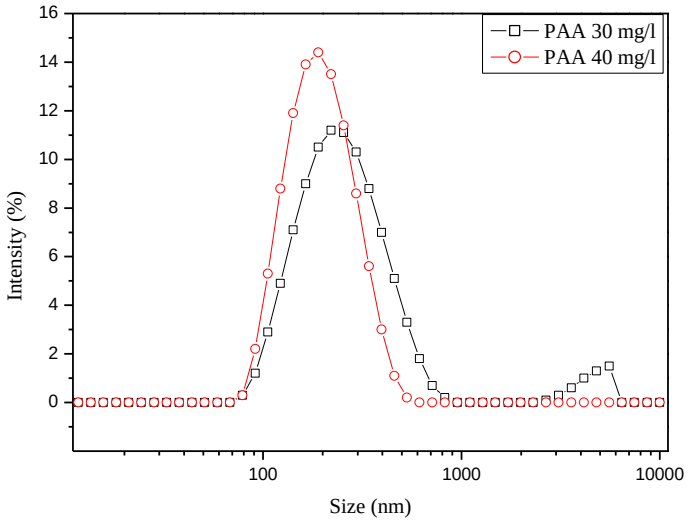

Figure 11: Size distribution by intensity of alumina nanoparticles in suspensions with PAA after 180 s of ultrasonication.

Table 1: Temperature of suspensions at the end of ultrasonication (the initial temperature is 1 °C).

Vibration amplitude (%)	Mode (s/s)	Ultrasonic time (s)	T at the end of ultrasonication (°C)
10	Continuous	90	6
10	Pulsed 0.1/0.1	90	4
30	Continuous	30	8
30	Continuous	90	12
30	Pulsed 0.1/0.1	30	8
30	Pulsed 0.1/0.1	90	10
30	Pulsed 1.0/1.0	30	6
30	Pulsed 1.0/1.0	90	9
60	Continuous	90	24
60	Pulsed 0.1/0.1	90	20

Table 2 : Zeta potential and mean size of alumina nanoparticles in aqueous suspensions after 180 s of ultrasonication.

Solution	pH	Zeta Potential (mV)	Z-average (nm)	
			Continuous US	Pulsed US 0.1/0.1
H_2O	7.3	33.5±0.5	149.8±4.1	147.5±3.3
H_2SO_4	2.0	-0.3±0.5	flocculation	
HNO_3	2.3	50.9±2.2	143.1±2.5	142.4±2.7
KNO_3 0.01M	7.2	40.8±1.9	159.2±0.9	153.9±4.2
KNO_3 0.01M	2.3 (HNO_3)	51.9±1.3	147.9±3.1	144.9±2.3

Table 3 : Influence of PAA concentration on mean alumina particle sizes after 180 s of ultrasonication.

Concentration of PAA (mg/l)	Z-average (nm)	
	Continuous US	Pulsed US 0.1/0.1
0	149.8±4.1	147.5±3.3
10	flocculation	
20		
30	partial flocculation	
40	181.9±0.9	177.5±2.9
60	190.6±1.5	189.8±2.5
100	210.5±3.5	213.2±0.7